

Effect of Space Holder Size on Microstructure, Deformation and Corrosion Response of Ti4Al4Co (wt%) Alloy Foam

Pradeep Singh^{1,2}, Amit Abhash^{1,2}, Prashant Nair², Anup Khare², I B Singh^{1,2} & D P Mondal^{1,2*}

¹Academy of Scientific and Innovative Research, CSIR-Advanced Materials and Processes Research Institute, Bhopal 462 026, India

²CSIR- Advanced Materials and Processes Research Institute, Bhopal 462 026, India

Received 19 September 2018; accepted 15 January 2019

In the present study, Ti4wt%Al4wt%Co alloy foam has been made using mechanically alloyed powder and elemental powder through space holder technique to investigate the mechanical and corrosion behaviour. It is noted that after sintering, the average pore sizes are 65 μm , 128 μm and 196 μm for the foam samples made by the use of space holder sizes 75 μm , 152 μm and 220 μm , respectively. It is further noted that the reduction in pore size with respect to used space holder is higher for the foam made of elementary powder. The foam made of finer space holder exhibits greater relative density and less porosity. Because of this fact, it has higher plastic collapse stress or yield stress. The foam made with elementary powder exhibited higher strength than the foam made of milled powder. The foam made with coarser pore size exhibits less corrosion rate as compared to that one with finer pore size. The foam made with elementary powder attains higher corrosion rate as compared to that one made with milled powder.

Keywords: Ti Foam, Mechanical alloying, Pore size, Corrosion behaviour, Tafel plot

Introduction

Ti and its alloys are unique materials for bone replacement due to their favourable properties like light weight with high strength, biocompatibility and excellent corrosion resistance due to thin layer oxide formation on the surface^{1,2}. Despite having advantageous properties than other biomaterials, some problems remain persist with the Ti alloy bone replica. High elastic modulus of Ti alloy in comparison to the natural bone is one of the major problem that cause stress shielding effect, consequent bone resorption and failure of implant^{3,4}. Smooth surface of Ti alloy implant also causes the problem in osteointegration with fibre like tissues of the bone resulting implant loosening⁵. Also, relative movement of implant against natural bone in the medium of body fluid produces liberation of elemental ions and debris in the body that cause detrimental effect on the human health⁶.

Elastic modulus of the Ti alloy implant can be reduced by incorporation of pores in the bulk of the material known as porous material or foam. Ti alloys foam implant reduce the chance of stress shielding effect as well as improve the osteointegration between implant and the natural bone due to anchoring the

bone tissues in the pores of the implant. A popular method that can imparts the desired porosity up to the 90% is powder metallurgy route and space holder technique in which porosity can be tailored by choosing the appropriate amount of space holder. Materials that can be used as space holder are Ammonium bicarbonate⁷, Sodium chloride⁸, urea⁹, Magnesium¹⁰.

Mechanical alloying is a noble method for the grain refinement, uniform mixing and different phase formation at comparatively lower temperature. The refinement of powder particles is caused because of the fracturing, re-welding and re-fracturing processes due to impact among the powder particles and balls¹¹. In the present study, milled Ti4wt%Al4wt%Co powder was used as the base material for the manufacturing of foam. Ammonium bi carbonate of different particulate size was used as a space holder. The aim of this work was to investigate the effect of space holder size on the compressive strength of the foam. Also, corrosion behaviour of the foam is investigated for foams having different pore size and unmilled foam sample.

Experimental Procedure

Ti powder (99.9% pure) of irregular shape with average particle size 31 μm , 4 wt% circular shaped Al (99.8% pure and particle size < 20 μm) and 4 wt% Co

*Corresponding author (E-mail: mondalp@yahoo.com)

(99.5% pure and average particle size 36 μm) were taken as initial materials. Each material is supplied by Alpha Aesar Company, Germany. The constituents materials were mixed with stainless steel balls (diameter = 6mm) in proportion of 15 ball to Powder Ratio (BPR) in hardened steel cylindrical container of 250 mL volume. To perform wet milling, 5wt% of propanol and 50 mL distilled water also poured in the container as process controlling agent. Container was tightly sealed and clamped in horizontal high energy planetary ball mill for milling. Ball mill was operated at 200 rpm for 16 h. After completion of milling, whole milled mixture was taken out from the container and dried in an oven at 110 $^{\circ}\text{C}$ for 10 h to remove the water propanol solution. After drying, material was sieved to separate the balls from the milled powder.

Sieves that were used for straining the space holder, have sieve opening sizes of 105 μm , 150 μm , 200 μm and 300 μm . Three group of space holder were collected that have the size ranges <105 μm (S_1), 150-200 μm (S_2), 200-300 μm (S_3) (Proper information about space holder was summarized in Table 1). To make the foam, powder metallurgy route was adopted. Milled powder was vigorously mixed with ammonium bi carbonate (NH_4HCO_3) space holder of different sizes in volume proportion of 1:1. Small amount of (approximately 2 wt.%) PVA solution was also mixed to find strength in green compacts. Whole mixture was compacted by applying uniaxial load of 200 MPa in a cylindrical die made of hardened steel having diameter 12.7 mm. Three types of samples (M/S_1 , M/S_2 and M/S_3) were prepared by using milled powder and the space holder having three different sizes. One additional type of samples also compacted by using elemental powder ($\text{Ti}_4\text{wt}\%\text{Al}_4\text{wt}\%\text{Co}$) and the space holder having size S_3 in the proportion of 1:1 (sample is assigned as U/S_3). Compacted samples were dried in an oven at 150 $^{\circ}\text{C}$ up to 4 h to remove the space holder and PVA that impart pores. After drying, samples were sintered in high temperature vacuum furnace in two stages at 800 $^{\circ}\text{C}$ for 60 min and 1100 $^{\circ}\text{C}$ for 90 min.

Microstructures of milled and unmilled powders and prepared foams were investigated using Field Emission Scanning Electron Microscope (FESEM) of Nova Nano SEM 430 model. Elements present in the milled $\text{Ti}_4\text{Al}_4\text{Co}$ was investigated by using EDX that is additionally attached to the FESEM. Compressive test was carried out by using Instron (Model 8801) Universal Testing Machine (UTM) at strain rate of 0.001/s. Corrosion test was performed by a potentiostat using three conventional electrodes. Platinum wire was used as counter electrode while saturated calomel electrode as a reference electrode. Foam samples were employed as working electrode having exposed surface area of 0.188 cm^2 in the electrolyte. Simulated body fluid (SBF) was prepared by dissolving the different components of appropriate concentration in distilled water. The composition of the SBF is taken from somewhere¹².

Results and Discussion

Characterization of space holders

Frequency distribution curves for the particulates size of the space holders (SH) were shown in Fig. 1 (a-c). From the Fig. 1 (a), it is clear that the particulates size of SH varies from 45 μm to 105 μm in which 43% particulates' placing is between 75 to 90 μm of size range that was sieved by using the sieve having opening size 105 μm . Fig. 1 (b) indicates the frequency distribution curve for the particulates size of SH that was sieved between two sieve having sieve opening 150 μm and 200 μm . The range shown in the curve is well matched that varies between 145 μm to 200 μm . Major part of the SH lays between the size range of 165 μm to 175 μm that is 45% of the lot. Frequency distribution curve of SH that was sieved by using 200 μm and 300 μm sieve size is shown in Fig. 1 (c). The particulates that have the size between 230 μm to 260 μm , participate the major quantity that is about half of the total SH size. Average particulate sizes for the three group of SH were analysed as 75 μm , 152 μm and 220 μm for S_1 , S_2 and S_3 respectively (Table 1). Average major and minor dimensions of S_1 were observed as 87 μm and 60 μm while their value for S_2 were analysed as 152 μm and 117 μm , respectively.

Table 1 — Descriptions of used space holders (SH).

S.No.	Sieving range (μm)	Average particulate size (μm)	Average major dimension (μm)	Average minor dimension (μm)	Aspect ratio	SH group name
1	<105	75	87	60	1.45	S_1
2	150-200	152	152	117	1.54	S_2
3	200-300	220	268	155	1.73	S_3

Aspect ratio is an important factor that represents the shape of the particles in the form of sphericity. It is measured by dividing the average major dimension of the particles to the average minor dimension. The values of aspect ratio for S_1 , S_2 and S_3 were measured as 1.45, 1.54 and 1.73, respectively. It indicates that in this study, sphericity of the SH reduces with the increment of average size of the particulates.

XRD analysis of milled and unmilled powders

Milled powder (M) and unmilled powder mixture (U) were examined by XRD for identification of phase formation and change in crystallographic structures of the material due to milling. The XRD diffraction patterns of U and M were represented by the Fig. 2. The results show that U contains the peak

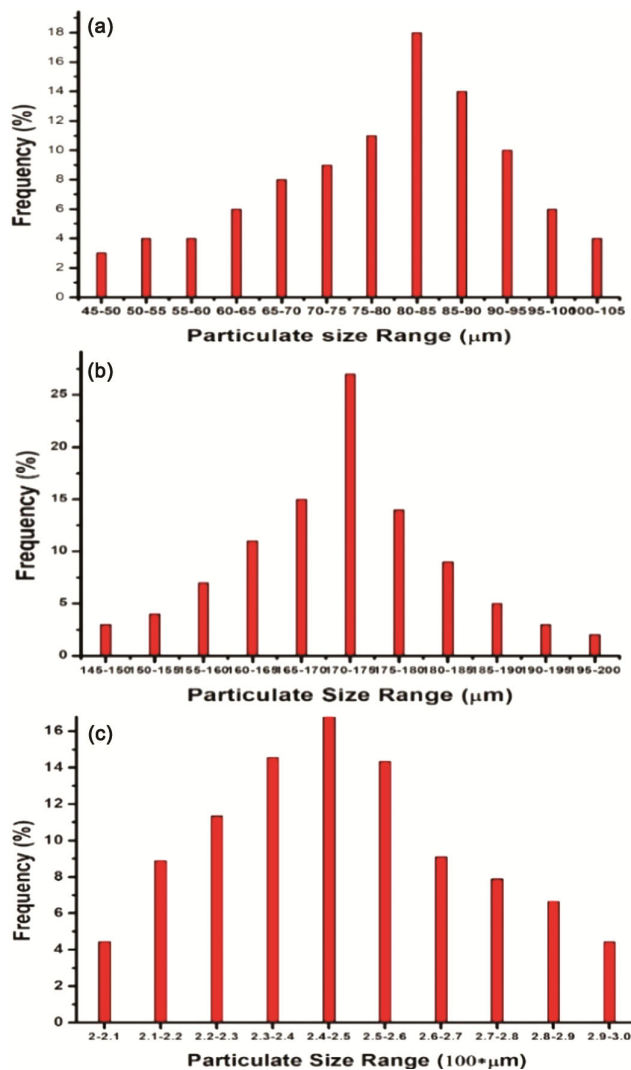


Fig. 1 — Frequency distribution curve for the average space holder size; (a) 75 μm , (b) 152 μm and (c) 220 μm .

of Ti, Al and Co as mixed. After milling, the possible phases in M that were analysed are α -Ti, TiO_2 and α (BCC) iron. Although in normal atmosphere, intense reaction of Ti and O to form TiO_2 takes place above 500 $^\circ\text{C}$ whereas during milling, reaction occurs at very low temperature (temperature of milling temperature could not exceed above 40 $^\circ\text{C}$). It may be caused due to generation of crystalline defects (grain boundary, dislocations, vacancy, stacking fault etc.) and new grain surface formation during milling that provide fast diffusion path and increase the kinetics of reaction. Peaks of α (BCC) iron also present in M as impurity because of wear of iron particles from the stainless steel container and balls due to impact, rolling and rubbing actions among them.

It is clear that TiO_2 was formed due to milling. Fe is present as impurity due to wear of the milling media. U has the peaks of as mixed elemental powder.

Microstructural analysis of powders

The micrographs of U and M obtained by FESEM were used for analyse the change in morphology, particle size distribution and average particle size of powder samples. Particle size distribution curves and respective microstructures of U and M were shown in Figs. 3 (a) and 3 (b), respectively. From the microstructure of Fig. 3 (a), it is clear that U has large size scattering ranges of particle with irregular shape. Particles have the size between 5 to 65 μm in which about 50% particles have the size in the range of 20 to 30 μm . Standard deviation indicates the scattering of the powder particles. For the sample U , it was measured as 12 that indicate the large scattering of the particles. Average particle size and aspect ratio of U were measured as 31 μm and 1.34, respectively.

The micrograph of M shows that the morphology of the powder particles got change due to milling. This

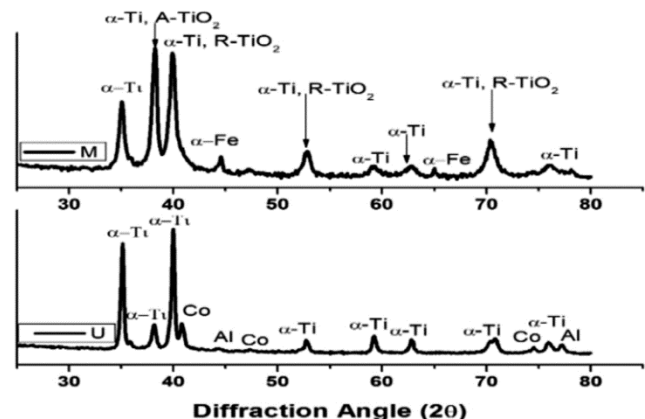


Fig. 2 — XRD analysis of the milled and unmilled powders.

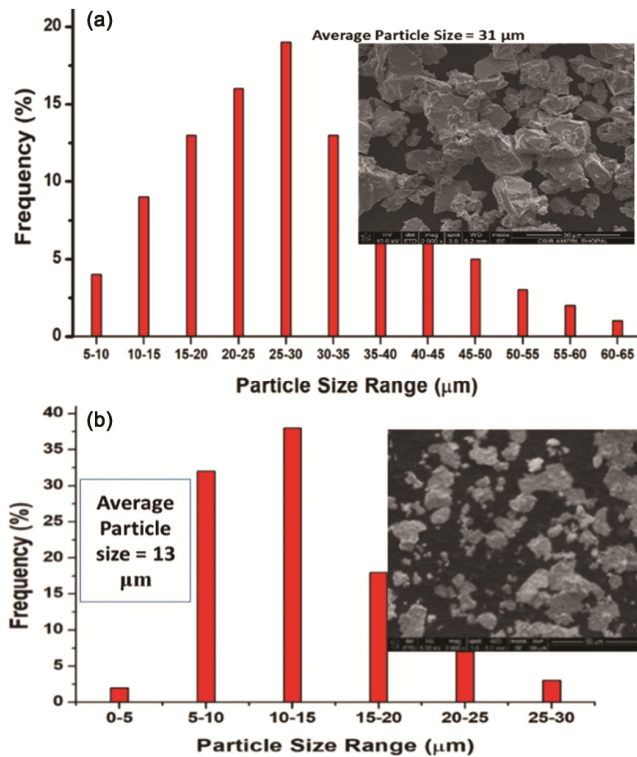


Fig. 3 — Frequency distribution curves for (a) powder U and (b) milled powder.

change occurs due to the rapid collision of stainless steel balls and the powder particle during milling in the high energy planetary ball mill. Range of particle size distribution reduces significantly in the range of 5 to 30 μm having standard deviation 5.36. Average particle size and aspect ratio of the milled powder M were measured as 13 μm and 1.56, respectively. Reduction in particle size range and hence average particle size is caused due to fracturing of particles because of the impact force imparts by the moving balls on the powder particles. Along with fracturing, particles got flattened that cause the increment in aspect ratio.

Microstructures of the foam samples

Densities of the samples were measured as 2.05 g/cc, 1.89 g/cc and 1.82 g/cc for the sintered samples M/S₁, M/S₂ and M/S₃ respectively (Sintered foam is shown in Fig. 4 (a)). The variation in densities of different foams is the difference in space holder size that was used to make the foam. The reason behind this is that the space holder particles having larger size form the larger interparticle voids during compaction. Microstructures of the M/S₁, M/S₂ and M/S₃ are shown in Figs. 4 (b, c and d) respectively. From the figures, it is clear that according to the descending order of number of pores per unit area

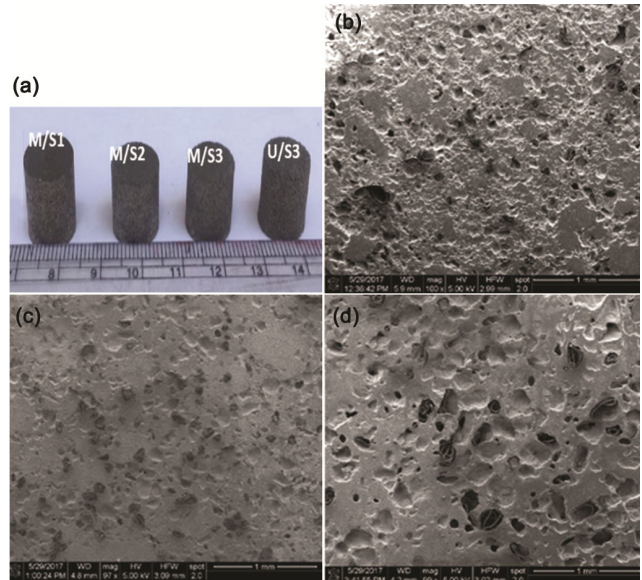


Fig. 4 — (a) Sintered foam samples, (b) micrographs of the foam samples M/S₁, (c) M/S₂ and (d) M/S₃.

accumulated by the foam samples is M/S₁, M/S₂ and M/S₃.

During formation of foam, the quantity of space holders used is same whereas size is varying. So, space holder of smaller size particulate has higher number of particulate resulting production of foam of higher number of pores. The average size of the pores for the foam samples M/S₁, M/S₂ and M/S₃ are calculated as 65 μm, 128 μm and 196 μm, respectively, that is 16.87%, 15.58% and 11.34% smaller than the average size of the space holders S₁, S₂ and S₃ that were mixed with powder during foam making. It is caused due to the shrinkage of the pores during sintering.

EDX analysis of the foams

The foam samples were characterized by the use of EDX to investigate the elements present in the foam material. Samples made with milled powder have impurities like iron, chromium, nickel and oxygen rather than used materials (Ti, Al, and Co). Iron, chromium and nickel exist due to wear of milling container and balls that were made of stainless steel material. Oxygen presents by the intensive reaction of titanium with air present in the container during milling. It was analysed that the amounts of present impurities are almost same for the M/S₁, M/S₂ and M/S₃ foams as given in Table 2. Existence of iron is advantageous for the foam in mechanical properties strengthening due to hindering the grain growth cause by the pinning action on the grain boundary during

Table 2 — EDX analysis of the of milled and unmilled foam samples.

S. No.	Foam sample name	Detected elements (wt%)						
		Ti	Al	Co	O	Fe	Cr	Ni
1	M/S ₁	53.16	3.77	3.71	27.61	8.45	1.87	1.43
2	M/S ₂	52.62	3.84	3.68	28.03	8.32	1.99	1.52
3	M/S ₃	52.42	3.98	3.76	28.26	7.96	2.01	1.61
4	U/S ₃	78.71	4.03	3.94	13.32	----	----	----

sintering by the formation of Fe₂Ti. Chromium and oxygen may help in improvement of corrosion resistance. Foam sample U/S₃ has the oxygen as impurity. The amount of oxygen in U/S₃ was analysed as the 57% lower in its value than the milled powder.

XRD analysis of the foams

XRD analysis of the foam materials were performed to investigate the phases formed after the sintering. For U/S₃, any intermetallic or precipitate formed among α -Ti, Al and Co was not detected in the XRD pattern as shown in Fig. 5. Formation of TiO₂ takes place due to the intense reaction of atmospheric oxygen with α -Ti during the any stage of foam sythesization. It was noted that the peaks of Al and Co were vanished after sintering. It is caused due to the solid solutionization of Al and Co in α -Ti lattice. Foam samples made by the use of milled powder (M/S₁, M/S₂ and M/S₃) have numerous phases of Ti and Fe. The formation of FeTi and Fe₂Ti was caused due to the limited solubility of iron in the α -Ti lattice. Some free α -Fe was also detected. Cr₂O₃, Ni₃Ti and α -Fe₂O₃ were also observed in small amounts. Because of rutile TiO₂ was traced at the peak having higher intensity in the pattern, shows considerable amount of TiO₂ formation after sintering.

Mechanical properties

In order to investigate the compressive properties, compression test of each foam sample was carried out. Fig. 6 (a) indicates the compressive stress-strain diagram of M/S₁, M/S₂ and M/S₃. It can be seen that the stress-strain curve is similar to the conventional foam. It has three regions known as elastic region, plateau region and densification region. In the elastic region, pores of the foam elastically deform. The maximum stress that can be sustained by the foam without collapsing the pores is known as plastic collapse stress. Above plastic collapse stress, pores of the foam collapse layer by layer and stress oscillate with small amplitude up to a certain limit of strain and a plateau of stress occurs. This region is known as plateau region of the foam. The average stress around

Table 3 — Mechanical properties of different foams.

Sample name	Maximum collapse stress (MPa)	Elastic modulus (GPa)	Plateau stress (MPa)	SEAC (MJ/m ³)
M/S ₁	79.64	26.38	19.41	11.4
M/S ₂	51.18	20.16	15.34	9.5
M/S ₃	38.22	15.79	11.62	7.1
U/S ₃	44.89	22.11	29.43	19.21

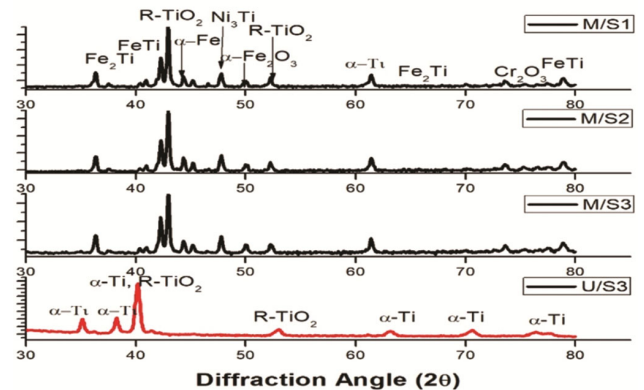


Fig. 5 — XRD analysis of the foam samples made by the use of milled and unmilled powder.

which oscillation takes place is known as plateau stress. After a certain strain, all the pores of the foam got collapse and it behaves as a solid material and stress increases drastically. The strain after which foam behaves as a solid material is known as the densification strain.

It is evident from the Fig. 6 (a) that plastic collapse stress of M/S₁, M/S₂ and M/S₃ are 79 MPa, 51 MPa and 38 MPa, respectively (The overall description of mechanical properties is given in Table 3). The value of elastic modulus is reported as 27 GPa, 21 GPa and 16 GPa for the respective M/S₁, M/S₂ and M/S₃ samples. It indicates that mechanical properties of the foam are strong function of relative density. A comparison was done between M/S₃ and U/S₃ to investigate the effect of milling on the mechanical properties of the foam. It was observed that the foam with made with unmilled powder has higher plastic collapse stress, elastic modulus, plateau stress and energy absorption capacity than the foam made with

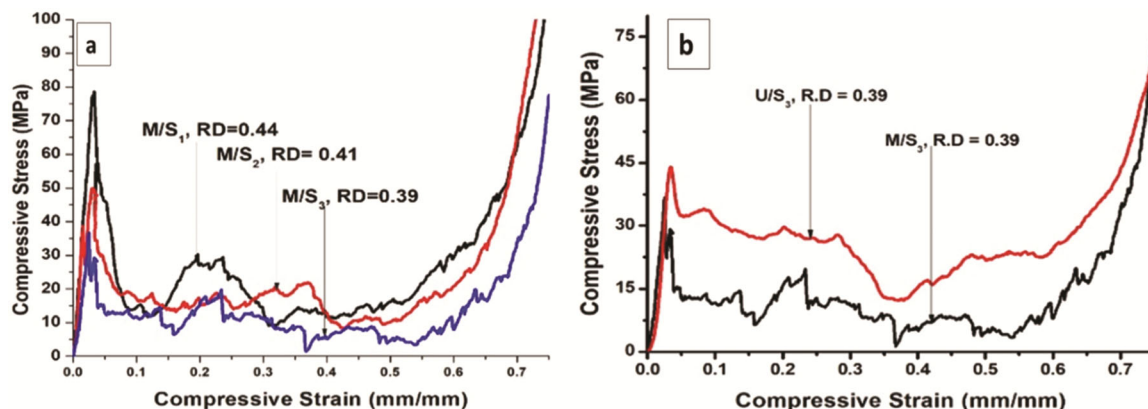


Fig. 6 — Stress- strain curves for (a) the foams made of milled powders having different pore sizes and (b) the foams made of milled and unmilled powders having same density.

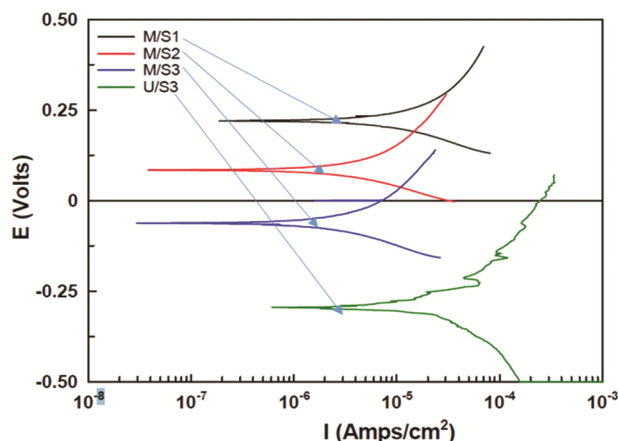


Fig. 7 — Tafel plot for foams made of milled and unmilled powders.

Table 4 — Corrosion properties of different foams.

Sample Name	E _{corr.} (V)	I _{corr.} ($\mu\text{A}/\text{cm}^2$)	Corrosion rate (mm/y)
M/S ₁	0.287	6.5	0.00234
M/S ₂	0.118	3.28	0.00186
M/S ₃	-0.014	1.17	0.00101
U/S ₃	-0.28	2.5	0.00139

milled powder Fig. 6 (b). It might be cause due to improper sinterability of milled powder due to containing higher amount of TiO₂.

Corrosion behaviour

To evaluate the corrosion behaviour of the milled foam having different size of pores, Tafel plot was drawn by the use of potentistat as shown in Fig. 7. The rate of corrosion for the M/S₁, M/S₂ and M/S₃ are 0.00234 mm/y, 0.00186 mm/y and 0.00101 mm/y, respectively (The summary of corrosion behaviour of the each foam is given in Table 4). This indicates that the foam of larger pore size has higher corrosion

resistance than the one with smaller pore size. It is caused due to the large number of pores available for the pitting and crevice corrosion. Also, M/S₃ has higher corrosion resistance than U/S₃. Because in U/S₃, alloying elements are not uniformly distributed and due to difference in electrochemical potential of each element, galvanic corrosion takes place while, in M/S₃ alloying elements are uniformly distributed in the material due to milling cause less chance of galvanic corrosion.

Conclusions

- (i) Microstructures of the foam samples indicate that average size of the pores is directly depend on the average size of used space holder during foam making.
- (ii) Foam sample that contains smaller pores has higher plastic collapse stress, elastic modulus and energy absorption capacity. Also, foam samples made with unmilled powder has higher mechanical properties than the foam sample made with milled powder having same density and pore size.
- (iii) The foam of larger pore size has higher corrosion resistance. Also, the foam made with milled powder has improved corrosion resistance than the foam made by the use of unmilled powder.

Acknowledgement

The authors gratefully acknowledged to Director, CSIR-AMPRI, Bhopal, India for giving permission to carry out the research experiment. Authors are also thankful to the co-ordinator AcSIR-AMPRI, Bhopal, India for granting permission to publish this work.

References

- 1 Albrektsson T, Brånemark P, Hansson H A, Kasemo B, Larsson K & Lundström I, *Annal Biomed Eng*, 11 (1983) 1.

- 2 Chu C, Chung C, Zhou J, Pu Y & Lin P, *J Biomed Mater Res Part A*, 75 (2005) 595.
- 3 Long M & Rack H, *Biomaterials*, 21 (1998) 1621.
- 4 Niinomi M, Hattori T, Morikawa K, Kasuga T, Suzuki A & Fukui H, *Mater Trans*, 43 (2002) 2970.
- 5 Lewis G, *J Mater Sci: Mater Med*, 24 (2013) 2293.
- 6 El Feninat F, Laroche G, Fiset M & Mantovani D, *Adv Eng Mater*, 4 (2002) 91.
- 7 Laptev A, Vyal O, Bram M, Buchkremer H & Stöver D, *Powder Metal*, 48 (2005) 358.
- 8 Bansiddhi A & Dunand D, *Acta Biomaterialia*, 4 (2008) 1996.
- 9 Sharma M, Gupta G, Modi O, Prasad B & Gupta A K, *Mater Lett*, 65 (2011) 3199.
- 10 Kim S W, Jung H D, Kang M H, Kim H E, Koh Y H & Estrin Y, *Mater Sci Eng C*, 33 (2013) 2808.
- 11 Suryanarayana C, *Rev Adv Mater Sci*, 18 (2008) 203.
- 12 Krzakała A, Służalska K, Widziołek M, Szade J, Winiarski A & Dercz G, *Electrochimica Acta*, 104 (2013) 407.